Proceedings of the 2004 IEEE
International Conference on Robotics & Automation
New Orleans, LA • April 2004

# Robust Multiple-Contact Postures in a Two-Dimensional Gravitational Field

Yizhar Or
Dept. of ME, Technion

Elon Rimon
Dept. of ME, Technion

*Abstract*— **We describe a practical method for computing the statically stable postures of a planar mechanism in a two-dimensional gravitational field. Our method lumps the complex kinematic structure of the mechanism into a rigid body $\mathcal{B}$ having a variable center of mass, while inertial forces generated by moving parts of the mechanism are lumped into a neighborhood of disturbance wrenches centered at the nominal gravitational wrench. Given this reduction, the statically stable postures of the mechanism correspond to center-of-mass locations of $\mathcal{B}$ that guarantee static stability for the neighborhood of wrenches. However, the response of $\mathcal{B}$ to an applied wrench involves dynamic ambiguity associated with different reaction modes at the contacts. Hence we compute only those center-of-mass locations where $\mathcal{B}$ maintains a non-ambiguous equilibrium for the entire neighborhood of wrenches. These center-of-mass locations are called the *robust stability region* of the posture. Focusing on two-contact postures, we compute the robust stability region as an arrangement of planar cells. Finally, we sketch an application of the results to robust locomotion planning of a 3-legged mechanism.**

## I. Introduction

Quasistatic locomotion of multi-legged mechanisms in a gravitational environment requires criteria for identifying and computing statically stable postures. This paper is concerned with the problem of identifying and computing the statically stable postures of a planar mechanism supported by multiple frictional contacts in a two-dimensional gravitational field. In order to simplify the problem, we lump the complex kinematic structure of the mechanism into a single rigid body $\mathcal{B}$ having a variable center of mass but maintaining the same contacts with the environment. Since free limbs of the mechanism must move during locomotion, we lump the inertial forces generated by moving parts into a neighborhood of disturbance wrenches (i.e. forces and torques) centered at the nominal gravitational wrench. Given this reduction, the statically stable postures of the original mechanism correspond to center-of-mass locations that guarantee static stability of $\mathcal{B}$.

Unfortunately, under the Coloumb friction law the dynamic response of $\mathcal{B}$ to an applied wrench can be ambiguous [6]. In order to eliminate such ambiguities, we rely on the practical criterion of strong stability [9]. By definition, $\mathcal{B}$ is *strongly stable* with respect to an applied wrench if the contacts supporting the object can statically resist the applied wrench, such that all other reaction modes are dynamically infeasible. However, in our case $\mathcal{B}$ is subjected to a neighborhood of external wrenches rather than a single wrench. Hence we introduce the notion of robust stability. By definition, $\mathcal{B}$ is *robustly stable* with respect to a neighborhood of wrenches if it is strongly stable with respect to all wrenches in the neighborhood.

Thus our objective is as follows. Given a set of contacts and a neighborhood of wrenches centered at the gravitational wrench, we wish to identify the posture's *robust stability region,* which is all center-of-mass locations that guarantee robust stability of $\mathcal{B}$.

In the grasping literature, Rajan et al. noticed that under the Coloumb friction law, the contact reaction modes of an object to an applied wrench can be ambiguous [10]. Rajan's work has been extended and applied by Erdmann and Mason to object pushing and manipulation [3], [6]. Balkcom et al. applied the notion of strong stability to part insertion [1]. Our paper generalizes the notion of strong stability to robust stability, and presents the first application of these notions to multi-legged locomotion. In multi-legged locomotion, Mason et al. [7] introduced the idea of lumping the kinematic structure of a mechanism into a rigid body having the same contacts with the environment and a variable center of mass. However, they were concerned with frictionless contacts, while we are concerned with frictional contacts. Several researchers considered the use of contact compliance in order to resolve the ambiguous dynamics associated with the rigid body paradigm (e.g. [5]). However, this approach is not only computationally intensive, but the mechanics of compliance in the presence of friction is still being investigated in the solid mechanics literature [4]. In contrast, *the notions of strong and robust stability provide conservative criteria for posture stability that can be applied under the much simpler rigid-body paradigm.*

We focus in this paper almost entirely on two-contact postures. In the next section we characterize the center-of-mass locations that generate feasible equilibrium postures. In Section III we list the non-static contact modes that can arise in two-contact postures. In Section IV we characterize analytically and graphically

0-7803-8232-3/04/$17.00 ©2004 IEEE

the center-of-mass locations that make the non-static modes dynamically feasible, assuming that a specific wrench acts on $\mathcal{B}$. In Sections V and VI we generalize the results to neighborhoods of wrenches, and identify the *robust stability region* associated with a posture and neighborhood of wrenches. The robust stability region is an arrangement of planar cells which we compute with a standard line-sweep algorithm. The final section discusses application of the results to robust locomotion planning of a 3-legged mechanism.

## II. Feasible Equilibrium Region

We characterize $\mathcal{B}$'s center-of-mass locations that generate feasible two-contact equilibrium postures on a piecewise linear terrain. We use the following notation. The contacts supporting $\mathcal{B}$ are denoted $x_1$ and $x_2$ (Figure 1(a)), while $x$ denotes $\mathcal{B}$'s center of mass. $n_i$ denotes the unit normal at the $i^{th}$ contact, pointing away from the terrain. The forces acting on $\mathcal{B}$ at the contacts are denoted $f_1$ and $f_2$. The gravitational force acting on $\mathcal{B}$ is denoted $f_g$. The disturbance force and torque acting on $\mathcal{B}$ is denoted $f_d$ and $\tau_d$. The net external force acting on $\mathcal{B}$ is denoted $f_{ext}$, where $f_{ext} = f_g + f_d$ such that $\|f_d\| \ll \|f_g\|$. The net external torque acting about $\mathcal{B}$'s center of mass, denoted $\tau_{ext}$, is $\tau_{ext} = \tau_d$.

When an external wrench acts on $\mathcal{B}$, the static equilibrium condition is $f_1 + f_2 = -f_{ext}$ and $(x_1 - x)^T J f_1 + (x_2 - x)^T J f_2 = -\tau_{ext}$, where $J = \begin{bmatrix} 0 & 1 \\ -1 & 0 \end{bmatrix}$. When the object is supported by two frictional contacts, the Coulomb friction law states that each force $f_i$ must lie in a *friction cone*, denoted $C_i$. Let $\mu$ be the coefficient of friction, and let $f_i^n$ and $f_i^t$ be the normal and tangent components of $f_i$. Then $C_i = \{f_i : |f_i^t| \le \mu f_i^n,\ f_i^n \ge 0\}$. We also need the following equivalent friction cone terminology. Let $C_i^u$ and $C_i^w$ denote unit vectors along the two edges of $C_i$ (Figure 1(a)). Then the $i^{th}$ friction cone is also given by $C_i = \{f_i^u C_i^u + f_i^w C_i^w : f_i^u, f_i^w \ge 0\}$. The intersection point of the edges $C_1^u$ and $C_2^u$ is denoted $p_{uu}$, and the intersection point of the edges $C_1^w$ and $C_2^w$ is denoted $p_{ww}$.

Consider first the nominal gravitational load, $f_{ext} = f_g$ and $\tau_{ext} = 0$. In static equilibrium each contact force can vary freely inside its friction cone. The equilibrium condition implies that $f_g$ must pass through the intersection point of the forces $f_1$ and $f_2$. Since $f_g$ acts at $\mathcal{B}$'s center of mass, the center of mass must lie inside the infinite vertical strip spanned by the polygon $C_1 \cap C_2$. This strip, denoted $S_1$, is also the infinite vertical strip bounded by $p_{uu}$ and $p_{ww}$ (Figure 1(a)). However, $S_1$ does not capture the condition that the contact forces can only push on the object, $f_i^n \ge 0$ for $i = 1, 2$. To guarantee this, the intersection point of $f_1$ and $f_2$ must lie inside the infinite vertical strip bounded by $x_1$ and $x_2$, which is denoted $S_2$ (Figure 1(a)). The feasible equilibrium region associated with the nominal gravitational load is therefore $S_1 \cap S_2$ .

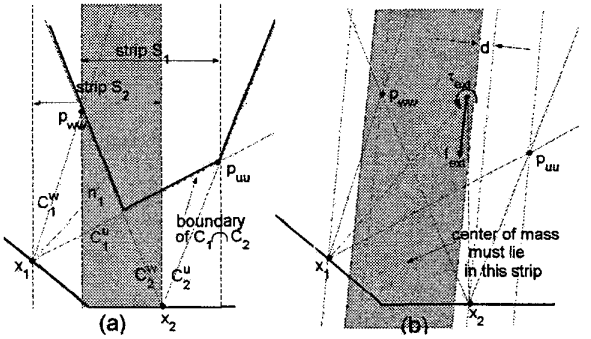


Fig. 1. (a) $\mathcal{R}_{ss} = S_1 \cap S_2$ for $f_{ext} = f_g$ and $\tau_{ext} = 0$. (b) $\mathcal{R}_{ss}$ for a general $(f_{ext}, \tau_{ext})$.

In the case of a general load, the feasible equilibrium region is constructed by rotating the strips $S_1$ and $S_2$ to match the direction of $f_{ext}$, then parallel shifting them by $-d$ where $d = \tau_{ext}/\|f_{ext}\|$ (Figure 1(b)).
The result is summarized as follows.

**Lemma II.1.** *Let an object $\mathcal{B}$ be supported by two frictional contacts and be subjected to an external wrench $(f_{ext}, \tau_{ext})$. The feasible equilibrium region, denoted $\mathcal{R}_{SS}$, is an infinite strip given by the intersection $\mathcal{R}_{SS} = S_1 \cap S_2$, where*

$$\begin{aligned} S_1 &= \{\, x : (x - p_{ww})^T J f_{ext} + \tau_{ext} < 0, \\ &\qquad (x - p_{uu})^T J f_{ext} + \tau_{ext} > 0 \,\} \\ S_2 &= \{\, x : (x - x_1)^T J f_{ext} + \tau_{ext} < 0, \\ &\qquad (x - x_2)^T J f_{ext} + \tau_{ext} > 0 \,\}, \end{aligned}$$

*where $x_1$ and $x_2$ are the contacts, and $p_{uu}$ and $p_{ww}$ are the left and right endpoints of $C_1 \cap C_2$.*

The lemma is consistent with the characterization of $\mathcal{R}_{SS}$ given in Ref. [3] in the context of object manipulation. Also, the lemma generalizes to $k$ contacts, in which case $\mathcal{R}_{SS}$ is still an infinite strip [8].

## III. The Non-Static Contact Modes

In this section we list the non-static contact modes, then review a key result: each combination of contact modes determines a unique dynamic response of $\mathcal{B}$.

**Classification of Contact Modes.** First consider a single frictional contact. In our case the object $\mathcal{B}$ is *initially at rest.* Hence the initial motion that $\mathcal{B}$ establishes at the contact is fully characterized by the contact force, $f_i$, and the relative acceleration of $\mathcal{B}$ at the contact, denoted $a_i$. Table I lists the contact modes that can arise for different combinations of $f_i$ and $a_i$, using the notation of Ref. [10]. In the table, $t_i$ denotes the unit tangent to the terrain at $x_i$, chosen such that $(t_i, n_i)$ is a right-handed pair. Note that each contact mode is associated with *two scalar equality constraints* in $f_i$ and $a_i$. The contact modes of $\mathcal{B}$ with respect to two simultaneous contacts are pairs of single-contact

| contact mode | physical meaning | kinematic constraints | force constraints |
|---|---|---|---|
| F | $\mathcal{B}$ breaks away at $x_i$ | $a_i \cdot n_i > 0$ | $f_i = \vec{0}$ |
| R (S) | $\mathcal{B}$ rolls about $x_i$ (or stationary at $x_i$) | $a_i = \vec{0}$ | $f_i^u > 0$ $f_i^w > 0$ |
| U | $\mathcal{B}$ slides along $t_i$ | $a_i \cdot n_i = 0$ $a_i \cdot t_i > 0$ | $f_i^u = 0$ $f_i^w > 0$ |
| W | $\mathcal{B}$ slides along $-t_i$ | $a_i \cdot n_i = 0$ $a_i \cdot t_i < 0$ | $f_i^w = 0$ $f_i^u > 0$ |

TABLE I
THE POSSIBLE CONTACT MODES AT A SINGLE FRICTIONAL CONTACT.

modes. For example, the contact mode UF means that $\mathcal{B}$ instantaneously slides along $t_1$ at $x_1$, while breaking contact at $x_2$. If we disregard the pairs' order and omit the kinematically infeasible pairs RW, RU, RR, UW (which occur only for special non-generic geometries), we are left with *six* contact modes: FF, UF, WF, RF, UU, and WW.

**Instantaneous Dynamic Solution.** Let $a \in \mathbb{R}^2$ and $\alpha \in \mathbb{R}$ denote the linear and angular acceleration of $\mathcal{B}$'s body frame located at its center of mass. The equations of motion of $\mathcal{B}$ under the influence of an external wrench and two contact forces are:

$$\begin{aligned} ma &= f_1 + f_2 + f_{ext} \\ I_c\alpha &= (x_1 - x)^T J f_1 + (x_2 - x)^T J f_2 + \tau_{ext}, \end{aligned} \quad (1)$$

where $m$ is $\mathcal{B}$'s mass, and $I_c$ is $\mathcal{B}$'s moment-of-inertia with respect to its center of mass. By assumption, $x_1$, $x_2$, $m$, and $I_c$ are known quantities. Thus, (1) consists of three scalar equations in the unknowns $f_1, f_2, a \in \mathbb{R}^2$ and $\alpha \in \mathbb{R}$, with $x$ acting as a free parameter. The following lemma asserts that the contact modes *uniquely* determine the unknown variables in terms of $x$. The lemma is stated for general $k$-contact postures.

**Lemma III.1 ([10]).** *Let an object $\mathcal{B}$ be supported by $k$ frictional contacts and be initially at rest. If $\mathcal{B}$ is subjected to an external wrench, any combination of contact modes at the $k$ contacts uniquely determines the initial contact forces and contact accelerations as a function of $\mathcal{B}$'s center of mass $x$.*

Returning to two-contact postures, a specific contact-mode pair also imposes inequality constraints on $f_1, f_2$ and $a_1, a_2$. Since the solutions for $f_1, f_2$ and $a_1, a_2$ depend on $x$, the resulting inequalities in $x$ determine for each non-static mode the region of center-of-mass locations where this particular mode is feasible. These regions are characterized below.

## IV. THE STRONG STABILITY REGION

Our objective is to *remove* from $\mathcal{R}_{SS}$ the center-of-mass region where the non-static contact modes are dynamically feasible. Hence we must first characterize the feasible regions of the non-static contact modes. The six non-static modes can be classified into four types. Since the pairs UF,WF and UU,WW differ only by the direction of sliding, we only need to consider the contact modes FF, RF, UF, and UU. We explicitly consider the first three modes, and relegate the UU mode to Ref. [8].

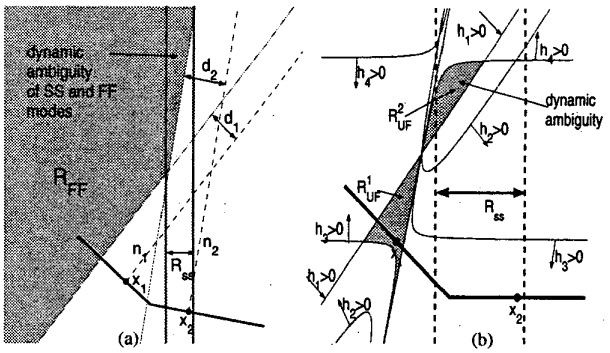


Fig. 2. (a) $\mathcal{R}_{SS}$ and $\mathcal{R}_{FF}$ for $f_{ext} = f_g$ and $\tau_{ext} > 0$. (b) $\mathcal{R}_{UF}$ inequalities for $f_{ext} = f_g$ and $\tau_{ext} > 0$.

### A. The Non-Static Feasible Regions

**The FF Feasible Region.** In the FF mode $\mathcal{B}$ instantaneously breaks away at both contacts. The equality constraints of this mode are $f_1 = f_2 = \vec{0}$, and the inequality constrains are $n_i \cdot a_i > 0$ for $i = 1, 2$. The following lemma characterizes the FF feasible region, which is denoted $\mathcal{R}_{FF}$.

**Lemma IV.1 ([8]).** *Let $\mathcal{B}$ be supported by two frictional contacts and be subjected to an external wrench $(f_{ext}, \tau_{ext})$. Then the FF feasible region is a semi-infinite polygon bounded by two edges, given by*

$$\mathcal{R}_{FF} = \{x : \tfrac{I_c}{m} f_{ext} \cdot n_i - \tau_{ext}(x - x_i) \cdot t_i > 0,\ i = 1, 2\}.$$

Note that $\mathcal{R}_{FF}$ depends on the inertia parameters of $\mathcal{B}$. Graphically, the $i^{th}$ edge of $\mathcal{R}_{FF}$ is parallel to $n_i$, and is shifted from $x_i$ along $t_i$ by a distance $d_i = -\frac{I_c}{m} |f_{ext} \cdot n_i| / \tau_{ext}$ (Figure 2(a)). Note that $\mathcal{R}_{FF}$ may intersect $\mathcal{R}_{SS}$, implying *dynamic ambiguity* of the SS and FF modes.

**The RF Feasible Region.** In the RF mode $\mathcal{B}$ instantaneously rolls at $x_1$ and breaks contact at $x_2$. The equality constraints of this mode are $a_1 = \vec{0}$ , $f_2 = \vec{0}$. The significant inequality constraint of this mode is $a_2 \cdot n_2 > 0$. However, the following lemma asserts that the RF feasible region is disjoint from $\mathcal{R}_{SS}$.

**Lemma IV.2 ([8]).** *Let $\mathcal{B}$ be supported by two frictional contacts and be subjected to an external wrench. Then the RF feasible region is always disjoint from the equilibrium region $\mathcal{R}_{SS}$.*

**The UF Contact Mode Region.** In the UF mode $\mathcal{B}$ instantaneously slides at $x_1$ along $t_1$, and breaks contact at $x_2$. The equality constraints of this mode are $f_2 = \vec{0}$, $n_1 \cdot a_1 = 0$, and $f_1^u = 0$. The inequality constraints of this mode are $f_1^w > 0$, $n_2 \cdot a_2 > 0$, and $t_1 \cdot a_1 > 0$. The following lemma characterizes the UF feasible region, which is denoted $\mathcal{R}_{UF}$.

**Lemma IV.3 ([8]).** *Let $\mathcal{B}$ be supported by two frictional contacts and be subjected to an external wrench $(f_{ext}, \tau_{ext})$. Then with $x_1$ chosen as frame origin, $\mathcal{R}_{UF}$ is the union of two sets, $\mathcal{R}_{UF} = \mathcal{R}^1_{UF} \cup \mathcal{R}^2_{UF}$, given by*

$$\mathcal{R}^1_{UF} = \{x : \min_{i=1,2,3,4}\{h_i(x)\} > 0\}$$
$$\mathcal{R}^2_{UF} = \{x : \max_{i=1,2,3,4}\{h_i(x)\} < 0\},$$

*where $h_1(x) = m(t_1 \cdot x)\tau_{ext} - I_c(f_{ext} \cdot n_1)$, $h_2(x) = I_c(n_1 \cdot C_1^w) - m(t_1 \cdot x)x^T J C_1^w$, $h_3(x) = (n_1 \cdot x)h_0(x) + \frac{1}{m}((t_1 \cdot C_1^w)h_1(x) + (t_1 \cdot f_{ext})h_2(x))$, and $h_4(x) = t_2 \cdot (x - x_2)h_0(x) + \frac{1}{m}((n_2 \cdot C_1^w)h_1(x) + (n_2 \cdot f_{ext})h_2(x))$, s.t. $h_0(x) = (n_1 \cdot f_{ext})x^T J C_1^w + (n_1 \cdot C_1^w)\tau_{ext}$.*

Note that $h_1$ is linear in $x$, while $h_2, h_3, h_4$ are *quadratic* in $x$. The zero level-set of $h_i$ for $i = 2, 3, 4$ consists of two hyperbolic curves (Figure 2(b)).

### B. Computation of Strong Stability

Let us summarize the results. The feasible equilibrium region, $\mathcal{R}_{SS}$, is an infinite strip parallel to $f_{ext}$ and displaced from the contacts by a distance corresponding to $\tau_{ext}$. The strong stability region is obtained by *removing* from $\mathcal{R}_{SS}$ the feasible regions of the non-static modes. The following proposition summarizes the procedure for computing the strong stability region.

**Proposition IV.4.** *Let $\mathcal{B}$ be supported by two frictional contacts and be subjected to an external wrench $w = (f_{ext}, \tau_{ext})$. Then the strong stability region for the posture, denoted $\mathcal{R}(w)$, is given by $\mathcal{R}(w) = \mathcal{R}_{SS} - \mathcal{R}_{FF} \cup \mathcal{R}_{UU} \cup \mathcal{R}_{WW} \cup \mathcal{R}_{UF} \cup \mathcal{R}_{FU} \cup \mathcal{R}_{FW} \cup \mathcal{R}_{WF}$, where $\mathcal{R}_{WW}$ is obtained from $\mathcal{R}_{UU}$ by reversal of sliding direction, and $\mathcal{R}_{WF}, \mathcal{R}_{FU}, \mathcal{R}_{FW}$ are obtained from $\mathcal{R}_{UF}$ by reversal of sliding direction or exchange of contact indices.*

## V. Robust Stability Region

In this section and the next one we consider the computation of the *robust stability region*, defined as $\mathcal{R}(\mathcal{W}) = \cap_{w \in \mathcal{W}} \mathcal{R}(w)$, where $\mathcal{W}$ is a given neighborhood of disturbance wrenches and $\mathcal{R}(w)$ the strong stability region associated with $w$. First we describe a convenient parametrization for $\mathcal{W}$. Then we characterize the feasible equilibrium region associated with $\mathcal{W}$, which is denoted $\mathcal{R}_{SS}(\mathcal{W})$. In the next section we revisit the non-static contact modes, and compute the center-of-mass locations where these modes are dynamically feasible for *some* $w \in \mathcal{W}$. Finally, $\mathcal{R}(\mathcal{W})$ is obtained by removing from $\mathcal{R}_{SS}(\mathcal{W})$ the feasible regions of the non-static modes.

**The Disturbance Neighborhood $\mathcal{W}$.** Let $(f_x, f_y)$ denote the horizontal and vertical coordinates of $f_{ext}$. By construction, $f_{ext} = f_g + f_d$ such that $f_g$ is vertical and $\|f_d\| \ll \|f_g\|$. Hence $f_y \neq 0$, and we can define *homogeneous coordinates* for wrench space as $(p, q)$, where $p \triangleq \frac{f_x}{f_y}$ and $q \triangleq \frac{\tau_{ext}}{f_y}$. The $(p, q)$ coordinates can be interpreted as follows. The nominal gravitational load, $(f_{ext}, \tau_{ext}) = (f_g, 0)$, corresponds to $p = q = 0$. Any other wrench $(f_{ext}, \tau_{ext})$ can be represented by its magnitude and its oriented line of action. The wrench's line of action is oriented along $f_{ext}$, and the perpendicular distance of the line from $\mathcal{B}$'s frame origin is $\tau_{ext}$. Hence $p$ represents the orientation of the wrench's line of action. Since $\mathcal{B}$'s frame origin is at its center of mass, $q$ represents the horizontal distance from $\mathcal{B}$'s center of mass to the wrench's line of action. Using $(p, q)$, we assume that $\mathcal{W}$ is a *rectangular neighborhood* defined by $\mathcal{W} = \{(p, q) : -\kappa \leq p \leq \kappa, -\nu \leq q \leq \nu\}$, where $\kappa$ and $\nu$ are given positive parameters. Note that $\mathcal{W}$ remains a rectangular neighborhood for any choice of a fixed reference frame. Note, too, that the robust equilibrium region associated with $\mathcal{W}$ is automatically associated with wrenches of arbitrary magnitude whose line of action is parametrized by $\mathcal{W}$.

**The Feasible Equilibrium Region of $\mathcal{W}$.** Given a two-contact posture of $\mathcal{B}$ and a neighborhood of wrenches $\mathcal{W}$, the *feasible equilibrium region of $\mathcal{W}$*, $\mathcal{R}_{SS}(\mathcal{W})$, is the set of center-of-mass locations that generate a feasible equilibrium of $\mathcal{B}$ for *all* $w \in \mathcal{W}$. The following lemma characterizes this region.

**Lemma V.1 ([8]).** *Let $\mathcal{B}$ be supported by two frictional contacts and be subjected to a neighborhood $\mathcal{W} = [-\kappa, \kappa] \times [-\nu, \nu]$ of external wrenches. The feasible equilibrium region of $\mathcal{W}$ is the intersection of two parallelograms, $\mathcal{R}_{SS}(\mathcal{W}) = P_1 \cap P_2$, given by $P_1 = \{x : (x - p_{ww})^T J u - \nu > 0, (x - p_{uu})^T J u + \nu < 0\}$ and $P_2 = \{x : (x - x_1)^T J u - \nu > 0, (x - x_2)^T J u + \nu < 0\}$, where $u = (\pm\kappa, 1)$.*

The graphical characterization of $P_1$ and $P_2$ is as follows. Recall that $p_{uu}$ and $p_{ww}$ are the left and right endpoints of $\mathcal{C}_1 \cap \mathcal{C}_2$. Also recall that $\mathcal{R}_{SS}(\mathcal{W}) = S_1 \cap S_2$, such that $S_1$ is bounded by $p_{uu}$ and $p_{ww}$, and $S_2$ is bounded by $x_1$ and $x_2$. Now consider the parallelograms $\tilde{P}_1$ and $\tilde{P}_2$ obtained by *intersecting* the strips $S_1$ and $S_2$ with orientations varying in $[-\kappa, \kappa]$. The edges of these parallelograms form angles of $\pm\beta$ with respect to $-e$, where $\beta = \tan^{-1}(\kappa)$. The final parallelograms $P_1$ and $P_2$ are obtained by shifting the edges $\tilde{P}_1$ and $\tilde{P}_2$ *inward*, by a horizontal distance of $\nu$ (Figure 3).

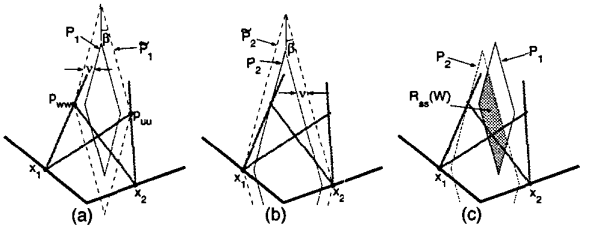


Fig. 3. (a)-(b) $P_1$ and $P_2$ for $\mathcal{W} = [-\kappa, \kappa] \times [-\nu, \nu]$, where $\beta = \tan^{-1}(\kappa)$. (c) $\mathcal{R}_{SS}(\mathcal{W}) = P_1 \cap P_2$.

## VI. The Robust Stability Region

The *$\mathcal{W}$-feasible region* of a non-static mode is defined as the *union* of the feasible regions associated with the individual wrenches in $\mathcal{W}$. We now characterize the $\mathcal{W}$-feasible region of the non-static modes. These modes were classified into four types: FF, RF, UF, and UU. However, Lemma IV.2 implies that the $\mathcal{W}$-feasible region of the RF mode is disjoint from $\mathcal{R}_{SS}(\mathcal{W})$. Hence we only need to consider the non-static modes FF, UF, and UU. Here, too, we relegate the UU mode to Ref. [8], and consider only the FF and UF modes.

First we review a projection technique that allows us to compute the $\mathcal{W}$-feasible regions. Let $\boldsymbol{p} = (p, q)$, and recall that $\boldsymbol{x}$ is $\mathcal{B}$'s center of mass. In Section IV we described the feasible regions of the non-static modes as inequalities in $(\boldsymbol{x}, \boldsymbol{p})$-space which can be identified with $\mathbb{R}^4$. Let $\mathcal{V}$ denote the feasible set of a specific non-static mode in $\mathbb{R}^4$. The wrench neighborhood $\mathcal{W}$ can be interpreted as a rectangular prism in $\mathbb{R}^4$. Hence the $\mathcal{W}$-feasible region of a particular mode is the *projection* of $\mathcal{V} \cap \mathcal{W} \subseteq \mathbb{R}^4$ onto the $\boldsymbol{x}$-plane. The following theorem is an adaptation of standard results to our purposes (e.g. [2, p. 102]).

**Theorem 1 (Silhouette Theorem).** *Let $\Pi : \mathbb{R}^4 \to \mathbb{R}^2$ be the projection $\Pi(\boldsymbol{x}, \boldsymbol{p}) = \boldsymbol{x}$. Let $\mathcal{S} = \{(\boldsymbol{x}, \boldsymbol{p}) \in \mathbb{R}^4 : f_1(\boldsymbol{x}, \boldsymbol{p}) \leq 0, \ldots, f_k(\boldsymbol{x}, \boldsymbol{p}) \leq 0\}$. Then $\Pi(\mathcal{S})$ is an arrangement of two-dimensional cells bounded by the projection of the silhouette curves of $\mathcal{S}$. Moreover, the silhouette curves consist of critical points of $\Pi$ on the boundary of $\mathcal{S}$.*

We use the silhouette theorem to obtain a description of the $\mathcal{W}$-feasible region of the non-static modes $FF$ and $UF$. Then we obtain the robust stability region by *removing* the cells of these modes from $\mathcal{R}_{SS}(\mathcal{W})$.

### A. The $\mathcal{W}$-Feasible Regions

**The FF Mode.** The following lemma describes the $\mathcal{W}$-feasible region of the FF mode, denoted $\mathcal{R}_{FF}(\mathcal{W})$.

**Lemma VI.1 ([8]).** *Let $\mathcal{B}$ be supported by two frictional contacts and be subjected to a neighborhood $\mathcal{W} = [-\kappa, \kappa] \times [-\nu, \nu]$ of external wrenches. Then $\mathcal{R}_{FF}(\mathcal{W})$ is the union of two semi-infinite polygons, $Q_1$ and $Q_2$, given by $Q_1 = \{\boldsymbol{x} : \rho(n_{iy} - |n_{ix}|\,\kappa) - \nu(\boldsymbol{x} - x_i) \cdot t_i < 0 \text{ for } i = 1, 2\}$ and $Q_2 = \{\boldsymbol{x} : \rho(n_{iy} - |n_{ix}|\,\kappa) + \nu(\boldsymbol{x} - x_i) \cdot t_i < 0 \text{ for } i = 1, 2\}$, where $n_i = (n_{ix}, n_{iy})$ and $\rho = \frac{I_c}{m}$.*

An example of $\mathcal{R}_{FF}(\mathcal{W})$ is shown in Figure 4(a). In the proof, we convert the $\mathcal{R}_{FF}$ inequalities of Lemma IV.1 into $(p, q)$ coordinates, together with the wrench inequalities $|p| \leq \kappa$ , $|q| \leq \nu$. Next we project the obtained set in $\mathbb{R}^4$ onto the $\boldsymbol{x}$-plane. Finally, application of Theorem 1 yields the silhouette curves.

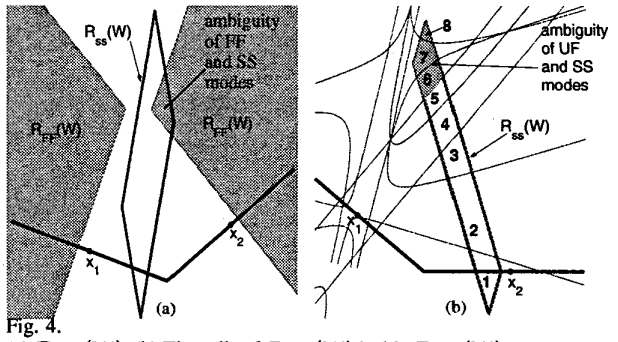


Fig. 4.
(a) $\mathcal{R}_{FF}(\mathcal{W})$. (b) The cells of $\mathcal{R}_{UF}(\mathcal{W})$ inside $\mathcal{R}_{FF}(\mathcal{W})$ are $6, 7, 8$.

**The UF Mode.** The $\mathcal{W}$-feasible region of the UF mode, denoted $\mathcal{R}_{UF}(\mathcal{W})$, is described in the following lemma.

**Lemma VI.2 ([8]).** *Let $\mathcal{B}$ be supported by two frictional contacts and be subjected to a neighborhood $\mathcal{W} = [-\kappa, \kappa] \times [-\nu, \nu]$ of external wrenches. Let $n_i = (n_{ix}, n_{iy})$ and $t_i = (t_{ix}, t_{iy})$. Then $\mathcal{R}_{UF}(\mathcal{W})$ is an arrangement of planar cells bounded by the curves:*

$$h_1(\boldsymbol{x}) = \pm\nu m(t_1 \cdot \boldsymbol{x}) - I_c(\pm\kappa n_{1x} + n_{1y}) = 0$$
$$h_2(\boldsymbol{x}) = I_c(n_1 \cdot C_1^w) - m(t_1 \cdot \boldsymbol{x})\boldsymbol{x}^T J C_1^w = 0$$
$$h_3(\boldsymbol{x}) = (n_1 \cdot \boldsymbol{x})h_0(\boldsymbol{x}) + \tfrac{1}{m}(t_1 \cdot C_1^w)h_1(\boldsymbol{x}) + \tfrac{1}{m}(\pm\kappa t_{1x} + t_{1y})h_2(\boldsymbol{x}) = 0$$
$$h_4(\boldsymbol{x}) = t_2 \cdot (\boldsymbol{x} - x_2)h_0(\boldsymbol{x}) + \tfrac{1}{m}(n_2 \cdot C_1^w)h_1(\boldsymbol{x}) + \tfrac{1}{m}(\pm\kappa n_{2x} + n_{2y})h_2(\boldsymbol{x}) = 0,$$

*where $h_0(\boldsymbol{x}) = (\pm\kappa n_{1x} + n_{1y})\boldsymbol{x}^T J C_1^w \pm \nu(n_1 \cdot C_1^w)$.*

In order to complete the computation of $\mathcal{R}_{UF}(\mathcal{W})$, we must identify which cells in the arrangement formed by the curves specified in the lemma belong to $\mathcal{R}_{UF}(\mathcal{W})$. The cells are bounded by quadratic curves, and they can be efficiently identified using an adaptation of the standard line-sweep algorithm. This algorithm generates a sample point $\boldsymbol{x}_0$ for each cell. Now a key step is to observe that the inequalities $h_i(\boldsymbol{x}_0, \boldsymbol{p}) > 0$ are *linear* in $\boldsymbol{p}$. Hence the problem of deciding whether a given cell with a sample point $\boldsymbol{x}_0$ belongs to $\mathcal{R}_{UF}(\mathcal{W})$ reduces to the standard linear programming problem of deciding if the $\boldsymbol{x} = \boldsymbol{x}_0$ linear system has a feasible solution $\boldsymbol{p}$. Figure 4(b) shows an example of running the line-sweep algorithm. The algorithm identifies eight cells inside $\mathcal{R}_{SS}(\mathcal{W})$, of which cells $6, 7, 8$ belong to $\mathcal{R}_{UF}(\mathcal{W})$.

### B. Computation of Robust Stability

The robust stability region, denoted $\mathcal{R}(\mathcal{W})$, is obtained by *removing* from $\mathcal{R}_{SS}(\mathcal{W})$ the $\mathcal{W}$-feasible regions of the non-static modes. The following corollary to Proposition IV.4 summarizes this final stage.

**Corollary VI.3.** *Let $\mathcal{B}$ be supported by two frictional contacts and be subjected to a neighborhood $\mathcal{W} = [-\kappa, \kappa] \times [-\nu, \nu]$ of external wrenches. Then the posture's robust stability region is given by*

$$\mathcal{R}(\mathcal{W}) = \mathcal{R}_{SS}(\mathcal{W}) - \mathcal{R}_{FF}(\mathcal{W}) \cup \mathcal{R}_{UU}(\mathcal{W}) \cup \mathcal{R}_{WW}(\mathcal{W}) \cup \mathcal{R}_{UF}(\mathcal{W}) \cup \mathcal{R}_{WF}(\mathcal{W}) \cup \mathcal{R}_{FU}(\mathcal{W}) \cup \mathcal{R}_{FW}(\mathcal{W}),$$

*where $\mathcal{R}_{WW}$ is obtained from $\mathcal{R}_{UU}$ by reversal of sliding direction, and $\mathcal{R}_{WF}, \mathcal{R}_{FU}, \mathcal{R}_{FW}$ are obtained from $\mathcal{R}_{UF}$ by reversal of sliding direction or exchange of contact indices.*

As a final example, let $\rho = \sqrt{I_c/m}$ be $\mathcal{B}$'s *radius of gyration.* Figure 5 shows the robust stability region for a specific posture with unit distance between $x_1$ and $x_2$, a neighborhood $\mathcal{W}$ given by $|\nu| \leq 0.1$ and $|\kappa| \leq \tan^{-1}(10°)$, and a coefficient of friction $\mu = 0.5$. Figure 5(a) shows that $\mathcal{R}(\mathcal{W})$ is identical to $\mathcal{R}_{SS}(\mathcal{W})$ for $\rho = 0.25$. However, dynamic ambiguity becomes more pronounced as $\rho$ decreases. Figures 5(b)-(c) show a gradual shrinking of $\mathcal{R}(\mathcal{W})$ for $\rho = 0.1$ and $\rho = 0.05$, due to dynamic ambiguity of the SS mode with the FF, UF, and FW modes.

## VII. Robust Locomotion Planning

In this last section we describe initial progress toward application of robust stability to quasistatic locomotion of a 3-legged robot in a planar environment. Rather than plan the mechanism detailed motion, we focus on planning a series of *footholds and center-of-mass locations* that bring the mechanism from start to target. We assume that the robot moves with a 2-3-2 gait pattern: during a two-contact phase the robot lifts a free leg to a new position while the supporting contacts remain stationary; during a three-contact transition phase the robot moves its center of mass while all three contacts remain stationary. Robust stability allows us to lump the inertial forces due to detailed motions of the mechanism into a neighborhood $\mathcal{W}$ of disturbance wrenches. Thus our objective is to plan a 2-3-2 gait in which the robot's center-of-mass continuously satisfies the *robust stability* criterion with respect to $\mathcal{W}$. In order to simplify the planning process, we require that the robot's center-of-mass execute a *straight line motion* during the three-contact transition phases. In Ref. [8] we prove that a straight-line motion of $\mathcal{B}$'s center-of-mass guarantees a feasible equilibrium with respect to $\mathcal{W}$ during the entire three-contact transition stage between two successive feasible equilibrium two-contact postures. Unfortunately the result does not readily extends to robust stability, since the $\mathcal{W}$-feasible regions of the non-static contact modes are inherently non-convex. However, in Ref. [8] we also prove that for each contact mode, checking that it is *infeasible* for $\lambda \in [0,1]$ reduces to checking the sign of at most five quadratic functions of the form $h_i(\lambda) = c_2^i\lambda^2 + c_1^i\lambda + c_o^i$ on the unit interval—a simple test of O(1) computation time.

To summarize, by making certain simplifying assumption on the motion of $\mathcal{B}$'s center of mass, robust stability for all phases of a 2-3-2 locomotion gait can be efficiently verified. Other motion planning issues such as foothold reachability and leg selection will be discussed in a future paper dedicated to this subject.

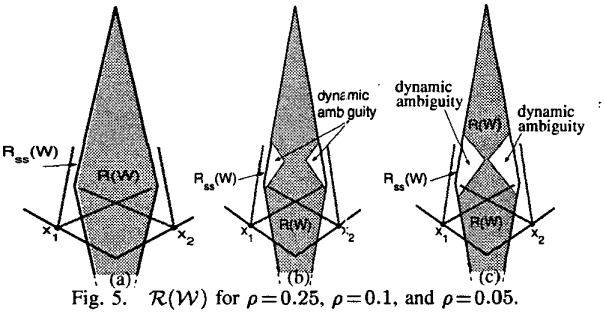

Fig. 5. $\mathcal{R}(\mathcal{W})$ for $\rho = 0.25$, $\rho = 0.1$, and $\rho = 0.05$.

## VIII. Concluding Discussion

Robust stability lumps the inertial forces generated by a moving mechanism into a neighborhood of disturbance wrenches acting on a rigid body having a variable center of mass. Focusing on two-contact postures, we characterized the center-of-mass locations where the dynamics of the equivalent rigid body is guaranteed to statically resist the entire neighborhood of wrenches. As a locomotion planning tool, one can focus on selecting foothold and center-of-mass locations that satisfy robust stability throughout the mechanism's motion. We described initial progress toward this application that involves robust 2-3-2 locomotion of a 3-legged robot. Our current research includes development of a full robust stability locomotion planner, as well as locomotion experiments on our 3-legged robot prototype (see www.technion.ac.il/~robots). Finally, the extension of robust stability to higher number of contacts in two-dimensions is discussed in Ref. [8].

## References


[1] D. J. Balkcom, E. J. Gottlieb, and J. C. Trinkle. A sensorless insertion strategy for rigid planar parts. In *IEEE Int. Conf. on Robotics and Automation*, pages 882–887, 2002.

[2] J. F. Canny. *The complexity of robot motion planning*. MIT Press, Cambridge, MA, 1988.

[3] M. A. Erdmann. An exploration of nonprehensile two-palm manipulation. *The Int. J. of Robotics Research*, 17(5), 1998.

[4] K. L. Johnson. *Contact Mechanics*. Cambridge Univ. Press, 1985.

[5] P. R. Kraus, V. Kumar, and P. Dupont. Analysis of frictional contact models for dynamic simulation. In *IEEE Int. Conf. on Robotics and Automation*, pages 2822–2827, 1998.

[6] M. T. Mason and Y. Wang. On the inconsistency of rigid-body frictional planar mechanics. In *IEEE Int. Conf. on Robotics and Aut.*, pages 524–528, 1988.

[7] R. Mason, J. W. Burdick, and E. Rimon. Stable poses of three-dimensional objects. In *IEEE Int. Conf. on Robotics and Automation*, pages 391–398, 1997.

[8] Y. Or and E. Rimon. Robust multiple-contact postures in a two-dimensional gravitational field. Tech. report, Dept. of ME, Technion, http://www.technion.ac.il/~robots, March 2003.

[9] J. S. Pang and J. C. Trinkle. Stability characterizations of fixtured rigid bodies with coulomb friction. In *IEEE Int. Conf. on Robotics and Automation*, pages 361–368, 2000.

[10] V. T. Rajan, R. Burridge, and J. T. Schwartz. Dynamics of rigid body in frictional contact with rigid walls. In *IEEE Int. Conf. on Robotics and Automation*, pages 671–677, 1987.